Draft version December 9, 2019
Typeset using LaTeX default style in AASTeX62

The Initial-Final Mass Relation

Meghan Cilento, Mairead Heiger, and Helena Richie

ABSTRACT

In this study, we explore the relation between a star's initial (Zero Age Main Sequence) mass and the mass of the white dwarf that it forms, the Initial-Final Mass Relation (IFMR). We also investigate the IFMR's dependence on metallicity. Using stellar evolution tracks from MIST (Choi et al. 2016), we characterize the shape of the IFMR at metallicities ranging from [Fe/H] = -4.00 to [Fe/H] = +0.25 using the Theil-Sen estimator (Wikipedia contributors 2019). We also compare the IFMR fits from MIST to observational measurements of the IFMR at known metallicities, available in Cummings et al. (2018), analyze the differences between models and observation, and comment on the differences between our fitting routines and those implemented by Cummings et al. (2018).

1. INTRODUCTION

The Initial-Final Mass Relation (IFMR) relates the mass of a white dwarf with the mass of its progenitor at the start of its main sequence lifetime. The IFMR is important in the study of stellar evolution, as it provides a method of constraining the final stages of evolution. There are many factors governing mass loss in the final stages of a star's evolution, such as convection, overshoot, dredge-up, mass loss, and nuclear reaction rates, that make it difficult to constrain the IFMR (Cummings et al. 2018).

Though progress has been made in the IFMR over the last several decades, challenges still exist due to the limitations of photometric and spectroscopic observational techniques. White dwarfs are very faint - especially at higher masses, so complete samples are difficult to obtain. The increased availability of wide-field imagers and spectrographs has led to increased numbers of known white dwarfs in star clusters, allowing many groups, including Cummings et al., to present advancements of the IFMR.

Here we explore the IFMR, utilizing MIST evolutionary tracks for the purpose of comparing results to those published by Cummings et al. (2018). Our goal is to use the best-fit to both MIST models and data to quantify differences between model predictions and data, as well as determine the best-fit to MIST models of a single metallicity that best represents the data. By calculating the model fits and data fits as a function of metallicity, our analysis will also allow us to directly compare the predictions in IFMR behavior between our analysis and that of Cummings et al. (2018).

2. IFMR FITTING ROUTINE

In order to compare the overall IFMR behavior as a function of metallicity, it was necessary to generate best fits of the MIST models, as well as the observational data. We chose to fit the MIST IFMR in three metallicity ranges - High: [Fe/H] = +0.50 to [Fe/H] = −0.50. Mid: [Fe/H] = −0.75 to [Fe/H] = −1.75. Low: [Fe/H] = −2.00 to [Fe/H] = −4.00. This division allowed us to more accurately visualize the differences in IFMR behavior as a function of metallicity, as well as determine the best fit to the observational data. We also make a qualitative cut at $M_i = 2.85 M_\odot$ to account for the non-linearity of the models and data, so our fits are piecewise linear relations.

We chose to use the Theil-Sen method to fit our IFMRs, because this routine is robust to outliers that exist in the models and observational data. Available through SciPy (scipy.stats.mstats.theilslopes()), this linear fitting method fits a line to a sample of points in the plane by choosing a median of the slopes of all lines through pairs of points (Wikipedia contributors 2019). The code for our fitting routine may be found in the provided iPython Notebook titled "Stars_Final_Project (IFMR).ipynb" under the sections "MIST IFMR fits with Theil-Sen method" and "Data Fitting with Theil-Sen method." The final results of our fits are shown in Figures 1, 2, and 3.

3. MIST PREDICTIONS

Based on the calculated IFMR of MIST models and observational data, we now present the equations of the overall linear fit and the linear fits for each metallicity group considered. These equations are in Table 1.

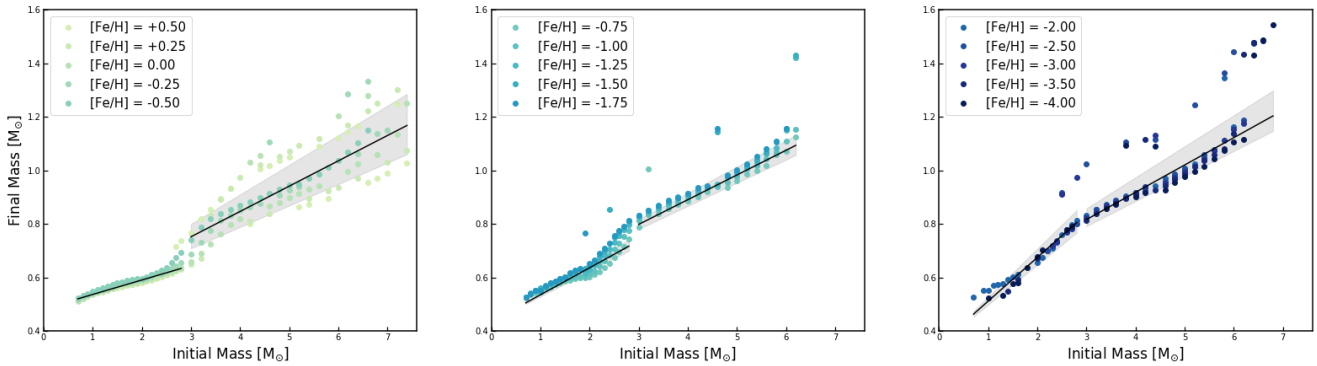

Figure 1: IFMR fits of MIST models in each of three metallicity ranges. The solid black lines represent the best fit for each metallicity range, and the shaded regions represent the lower and upper limits of the fits.

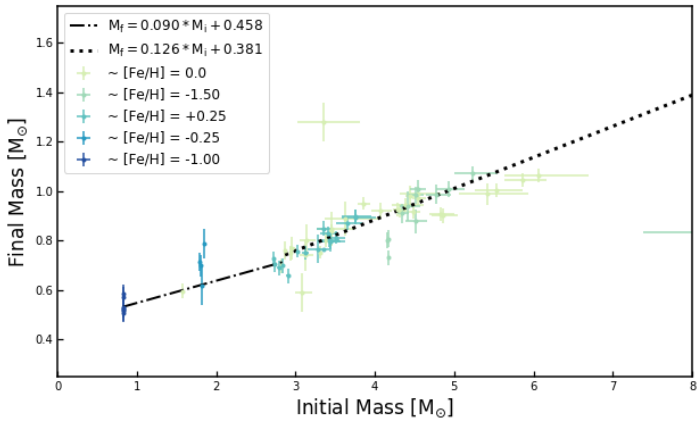

Figure 2: Cummings et al. (2018) semi-impirical data. Overlaid is our IFMR fit generated for the entire dataset.

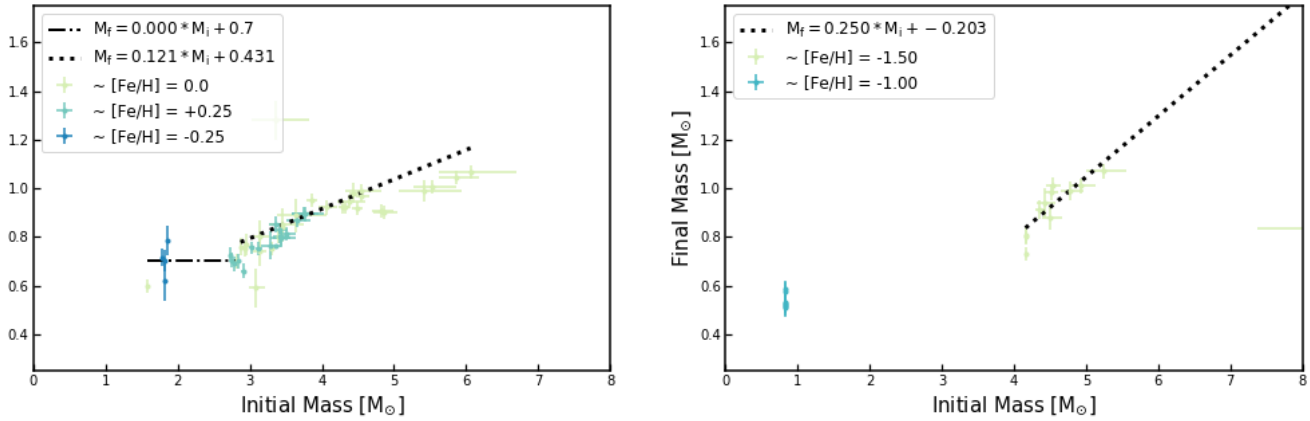

Figure 3: Cummings et al. (2018) semi-impirical data. Overlaid is our IFMR fit for two metallicity ranges. High (left): [Fe/H] = +0.50 to [Fe/H] = −0.50. Mid (right): [Fe/H] = −0.75 to [Fe/H] = −1.75. The dashed black lines represents the best fit to the data for each metallicity range. The low metallicity range ([Fe/H] < −2.00) is omitted because no observational data is available. Additionally, no fit exists in the mid metallicity range at masses below $2.85 M_{\odot}$ because the result is not statistically significant.

Table 1: IFMR Fit Results

MIST Fits		
Metallicity Range	IFMR ($M_i \leq 2.85\ M_\odot$)	IFMR (2.85 $M_\odot < M_i$)
Overall	$M_f = 0.0907^{+0.0096}_{-0.0107}\ M_i + 0.4321$	$M_f = 0.0978^{+0.0067}_{-0.0071}\ M_i + 0.5008$
[Fe/H] = +0.50 to [Fe/H] = −0.50	$M_f = 0.054^{+0.003}_{-0.003}\ M_i + 0.482$	$M_f = 0.098^{+0.007}_{-0.070}\ M_i + 0.501$
[Fe/H] = −0.75 to [Fe/H] = −1.75	$M_f = 0.101^{+0.009}_{-0.006}\ M_i + 0.434$	$M_f = 0.092^{+0.006}_{-0.006}\ M_i + 0.521$
[Fe/H] = −2.00 to [Fe/H] = −4.00	$M_f = 0.091^{+0.010}_{-0.011}\ M_i + 0.432$	$M_f = 0.102^{+0.016}_{-0.015}\ M_i + 0.5103$
Fits to observational data		
Metallicity Range	IFMR ($M_i \leq 2.85\ M_\odot$)	IFMR (2.85 $M_\odot < M_i$)
Overall	$M_f = 0.090^{+0.029}_{-0.020}\ M_i + 0.458$	$M_f = 0.126^{+0.018}_{-0.023}\ M_i + 0.381$
[Fe/H] = +0.50 to [Fe/H] = −0.50	$M_f = 0.000^{+0.092}_{-0.088}\ M_i + 0.7$	$M_f = 0.121^{+0.029}_{-0.023}\ M_i + 0.431$
[Fe/H] = −0.75 to [Fe/H] = −1.75	–	$M_f = 0.250^{+0.25}_{-0.19}\ M_i - 0.203$
[Fe/H] = −2.00 to [Fe/H] = −4.00	–	–

4. LITERATURE MEASUREMENTS

Cummings et al. (2018) presents the semi-empirical IFMR from Sirius B and 79 re-observed white dwarfs spanning progenitor masses of 0.85 to 7.5 $M_\odot$. The non-linearity of the Cummings et al. (2018) IFMR is clearly observable in their results (Figure 5 of Cummings et al. (2018)). To define the semi-empirical IFMR, they linearly fit the relation above and below the 2nd dredge-up turnover, which they determined to be at 3.60 $M_\odot$. By requiring these relations to be continuous, they created three equations for the MIST IFMR (Table 2), which are comparable to the equations generated by our own fits using the Theil-Sen method (Table 1).

Table 2: Literature IFMR Results

Cummings et al. 2018		
IFMR ($0.83 M_\odot < M_i < 2.85 M_\odot$)	IFMR ($2.85 M_\odot < M_i < 3.60 M_\odot$)	IFMR ($3.60 M_\odot < M_i < 7.20 M_\odot$)
$M_f = (0.080 \pm 0.016)\ M_i + (0.489 \pm 0.030)\ M_\odot$	$M_f = (0.187 \pm 0.061)\ M_i + (0.184 \pm 0.199)\ M_\odot$	$M_f = (0.107 \pm 0.016)\ M_i + (0.471 \pm 0.077)\ M_\odot$

5. COMPARISON & ANALYSIS

We note that the fits presented in (Cummings et al. 2018) are calculated using observed WD masses and theoretical ZAMS masses. To derive the initial masses, Cummings et al. (2018) fit MIST isochrones to the observational data of the clusters that contained the WDs to determine the age of the cluster as a whole. Once this semi-empirical IFMR had been determined, they used linear fitting methods to extract a three-part IFMR equation, which is shown in Table 2. So we are comparing both our semi-empirical IFMR (using their observed WD masses and theoretical ZAMS masses) and our purely theoretical IFMRs calculated using MIST models.

We see that the linear IFMR fit from Cummings et al. (2018), $M_f = (0.080 \pm 0.016) M_i + (0.489 \pm 0.030) M_\odot$, is in good agreement with our derived overall fit, $M_f = 0.090\ M_i + 0.458$, for $M_i \leq 2.85\ M_\odot$. By averaging the two-part IFMR equations from Cummings et al. (2018) for 2.85 $M_\odot < M_i$, we may directly compare our high-mass IFMRs. In our fitting routine, we derive the equation $M_f = 0.126\ M_i + 0.381$, while the Cummings high-mass fit is given by $M_f = 0.147\ M_i + 0.342$, which again, is in general agreement with our results. Since we used a unique fitting routine in this study, slight discrepancies between fits are expected, but the general agreement in overall IFMR shows that fitting robustly through the Theil-Sen method, rather than implementing data cuts to eliminate outliers, is a valid method of fitting to this data set.

In addition to directly comparing the IFMR fits to the data itself, we may compare the MIST IFMR fits to the fits to data corresponding to the metallicity ranges considered in this study. Figure 4 shows the linear fits to the IFMR of each metallicity available from MIST, as well as the observational data, to help visualize the metallicity fit which best represents the data. Provided in the iPython notebook in the section "MIST IFMR fits with Theil-Sen method" under "Best fit for each metallicity", we directly compare fit parameters to the fits of observational data (Figure 2)

and see that the individual fits to data by metallicity range are not well-represented by the MIST IFMR fits, which is expected based on the limited number of data points in each region for which the fit was generated. However, we do see that for the entire dataset, the low-mass region is well represented by the [Fe/H] = -1.00 fit (slope = 0.090, intercept = 0.446), and the high-mass region is well represented by the [Fe/H] = -0.25 fit (slope = 0.109, intercept = 0.407).

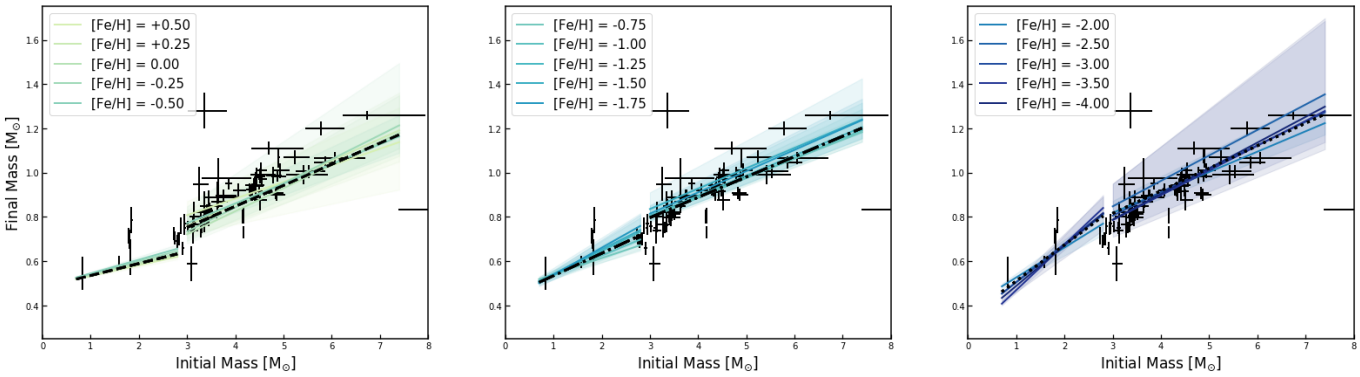

Figure 4: Linear fits to MIST IFMR in same the metallicity ranges used in Figure 1. The line of best-fit for each range of metallicities (black dashed line) and observational data from Cummings et al. (2018) are overlaid. Additionally, the upper and lower limit fits for each metallicity are shaded.

6. CONCLUSIONS

In general, we conclude that this study was not only successful in deriving IFMR fits of MIST evolutionary tracks, but it also demonstrates that the fitting routines implemented here are consistent with the published results of Cummings et al. (2018). It is clear that the overall trend of the IFMR is non-linear, which is reflected in the need to fit the IFMR in separate low and high mass regions to best characterize the data. Furthermore, the dependence of the IFMR on metallicity appears to depend on the mass range. The MIST fits at varying metallicity of higher mass stars have relatively constant slope, with intercept increasing as metallicity decreases. The MIST fits of varying metallicity of lower mass stars have slopes inversely related to metallicity – as metallicity decreases, the IFMR becomes steeper, but intercepts become constant. Additional observational data, however, is necessary to evaluate the accuracy of IFMRs of single metallicities from MIST. As survey technology improves, and we gather more white dwarf observations, it may be possible to fill in the gaps of the IFMR and truly identify a relation which clarifies the factors governing the final stages of stellar evolution. Until then, the use of semi-empirical IFMR models and stellar evolutionary models are necessary to deduce the IFMR.

REFERENCES

Choi, J., Dotter, A., Conroy, C., et al. 2016, ApJ, 823, 102

Cummings, J. D., Kalirai, J. S., Tremblay, P. E., Ramirez-Ruiz, E., & Choi, J. 2018, ApJ, 866, 21

Wikipedia contributors. 2019, Theil–Sen estimator — Wikipedia, The Free Encyclopedia, [Online; accessed 3-December-2019]